2015B1611 BL20XU

In-situ Imaging of Eutectic Growth in Electronic Solders

N. Hou[a], S.A. Belyakov[a], A. Sugiyama[b], H. Yasuda[c], C.M. Gourlay[a]

[a] Department of Materials, Imperial College, London,
[b] Dept. Mechanical Engineering for Transportation, Osaka Sangyo University,
[c] Dept. Materials Science and Engineering, Kyoto University

We directly image and measure unidirectional eutectic growth in electronic solders using synchrotron radiography on BL20XU. The dynamics of competitive growth between stable and metastable eutectics is studied in the Sn-Ni system and is compared with growth of the Sn-Cu_6Sn_5 and Sn-Ag_3Sn binary eutectics as well as the Sn-Ag_3Sn-Cu_6Sn_5 ternary eutectic.

Keywords : Pb-free soldering, electronic interconnections, eutectic growth, solidification.

Background and Objective :

Eutectic solidification is an important part of microstructure formation in electronic solder joints. Fig.1 shows a cross-section through a smart phone and the typical microstructure of a Cu/Ni(P)/Sn3.5Ag joint. It can be seen that more than 50% of the solder volume solidifies into a eutectic mixture which consists of ~95% βSn phase and ~5% of intermetallic compounds (Ag_3Sn and $NiSn_4$). Recently, we have shown that a metastable eutectic can form in Sn-rich Sn-Ni alloys [1][2]and also during electronic soldering of Sn-3.5Ag solder to Ni-based substrates [3]. In this case, the stable eutectic is βSn-Ni_3Sn_4 and the metastable eutectic is βSn-$NiSn_4$. The aim of this experiment was to directly image and measure the dynamics of competitive growth between the stable and metastable eutectic in the Sn-Ni system. We seek new insights into the mechanisms that enable the metastable eutectic to prevail over the stable eutectic during unidirectional solidification. A further aim was to compare the eutectic growth mechanisms of common eutectics in Pb-free soldering: Sn-Cu_6Sn_5, Sn-Ag_3Sn and the ternary Sn-Ag_3Sn-Cu_6Sn_5 eutectic.

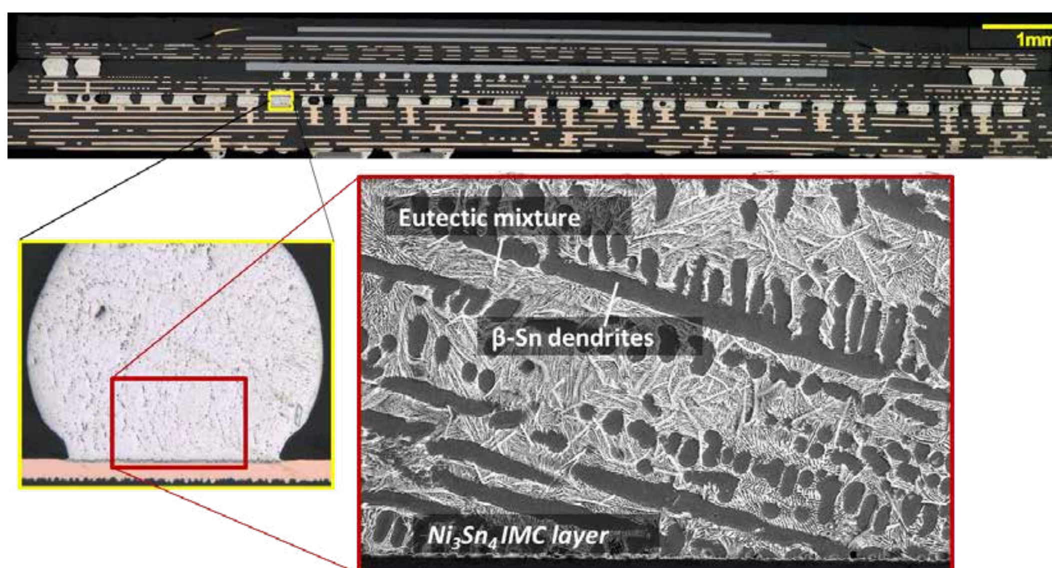

Fig.1. Cross-section through a smart phone and the typical microstructure of a Pb-free interconnect made using Sn-3.5wt%Ag solder on a Cu/Ni(P) surface finish.

Experiments :

Sn-rich Sn-Ni alloys were used to study the transitions between stable Sn-Ni_3Sn_4 and metastable Sn-$NiSn_4$ eutectic growth and Sn-Cu, Sn-Ag and Sn-Ag-Cu alloys were used to study Sn-Cu_6Sn_5, Sn-Ag_3Sn and Sn-Ag_3Sn-Cu_6Sn_5 eutectic growth. The compositions used were Sn-0.1Ni, Sn-0.15Ni and Sn-0.25Ni, Sn-0.9Cu, Sn-3.7Ag and Sn-3.7Ag-0.85Cu (all in mass%). Synchrotron radiography of vertical

unidirectional solidification was performed on BL20XU at Spring-8, using an X-ray energy of 16 keV. The techniques were based on those developed by Yasuda et al. [4]. The experiment rig is shown in Fig. 2a and the vertical motion stage provides pulling rates in the range 1 - 10 μm/s which were applied by pulling the sample downwards. The furnace was held at 400 ºC during all experiments. A thermocouple was inserted into the chamber to monitor the temperature. Fig. 2c shows setup of the sample and confining cell. 20 μm thick samples were used, confined within a 20 μm thick PTFE spacer cavity between SiO_2 sheets similar to (but thinner than) in ref. [5]. The field of view was ~1×1mm recorded with 0.502 μm per pixel at 1 frame per second with a 0.5 s exposure time using a CMOS camera.

Samples were initially pulled at 1 μm/s, were then increased to 5 or 10 μm/s and finally reduced back to 1μm/s. At all speeds, pulling was applied until a quasisteady-state growth microstructure formed. Actual interface velocities were tracked in the images. The temperature gradient in the liquid near the S-L interface was ~5 K/mm as measured with a Ø=0.1 mm B-type thermocouple in a separate experiment.

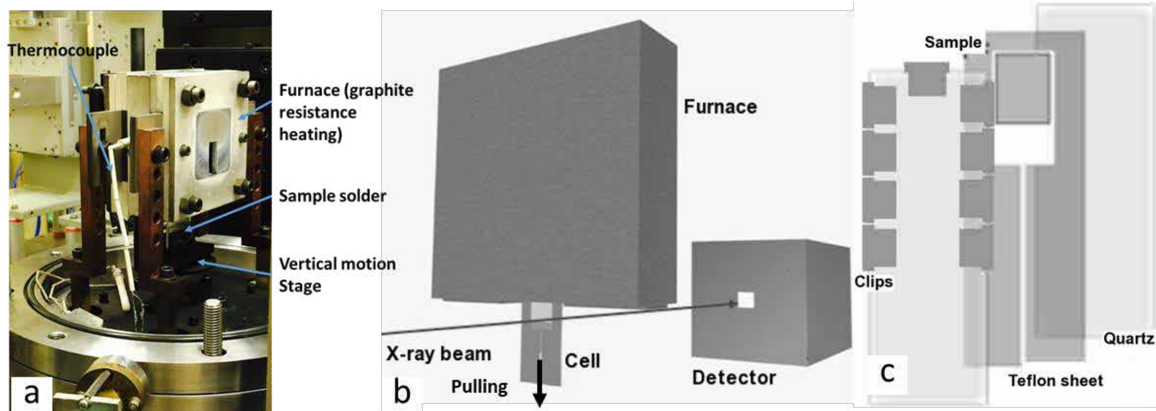

Fig.2. Experiment rig. (a) Unidirectional solidification rig; (b) Principle of synchrotron radiography; (c) Sample settings

Results and Discussion：

Steady state microstructures were grown for both the stable Sn-Ni_3Sn_4 and metastable Sn-$NiSn_4$ eutectics. Additionally, transitions between stable and metastable eutectic growth were successfully observed in Sn-0.1Ni, Sn-0.15Ni and Sn-0.25Ni. It was found that the transition from stable to metastable eutectic growth is reversible: increasing the growth rate from 1 - 5 um/s caused the stable to metastable transition and decreasing the growth rate from 5 - 1 um/s caused the metastable to stable eutectic transition. Fig. 3 shows the morphology at the transition between the two eutectics. Stable eutectic has a branched rod morphology and the metastable eutectic has a broken lamellae morphology.

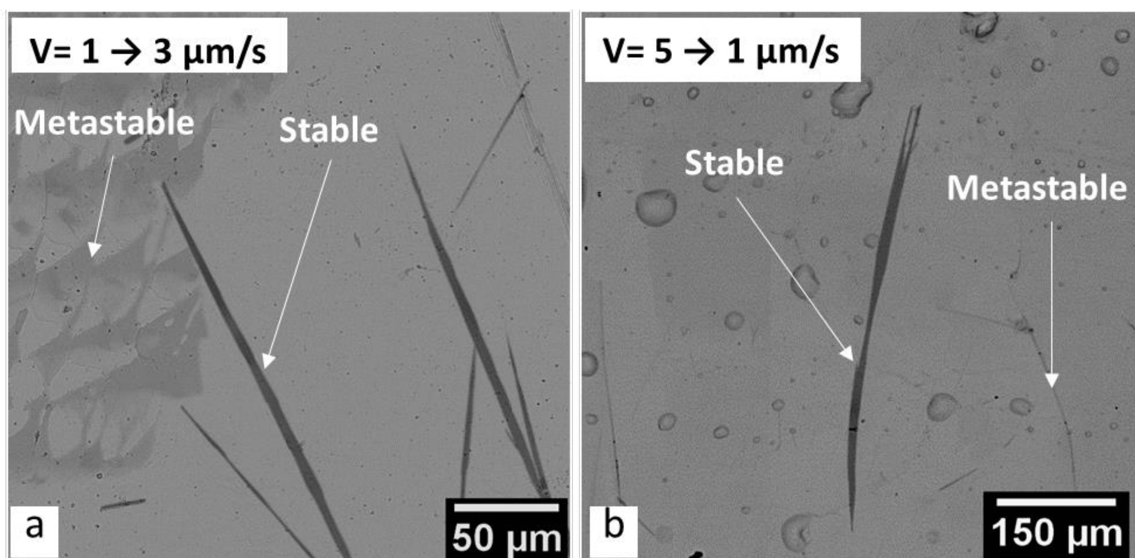

Fig.3. a. Transition from stable to metastable. b. Transition from metastable to stable eutectics in Sn-0.15Ni.

The kinetics of the transition were tracked in the image sequences, and the interface growth distance is plotted against time in Fig. 4. The red lines show the changing of pulling speed: 0, 1 μm/s, 10 μm/s, 1 μm/s, and 5 μm/s respectively. Blue solid lines indicate the regions of stable eutectic growth and blue dashed lines indicate the regions of metastable eutectic growth. At the beginning of 1 μm/s pulling, the stable and metastable eutectics start growing simultaneously. When the pulling speed increases to 10 μm/s, the stable eutectic stops growing and the metastable eutectic continues growing. After the pulling speed was changed back to 1 μm/s, the stable eutectic did not appear until 1400 s after the velocity change. The stable and metastable eutectics then grow at the same time for 2240 s and then the stable eutectic outcompetes the metastable eutectic. Finally, the interface velocity was increased again to 5 μm/s, and the metastable eutectic does not reappear due to the short growth distance remaining at the end of this experiment. An interesting feature in this and other datasets is that the time of the transition from stable to fully metastable eutectic is shorter than that from metastable to fully stable eutectic after a velocity change.

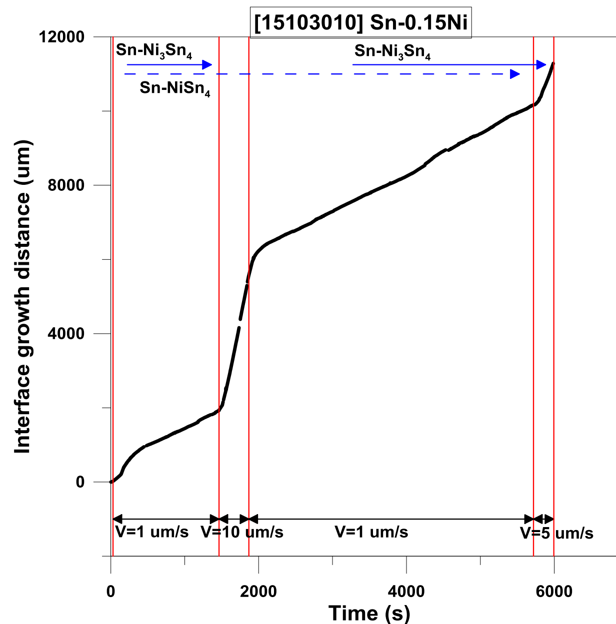

Fig.4. Plot of interface growth distance vs. time for Sn-0.15Ni

Fig.5(a) shows a typical region of stable Sn-Ni_3Sn_4 eutectic growth. Similar to other nonfaceted-faceted (nf-f) eutectics such as Al-Si, it is a highly “irregular” eutectic with an array of Ni_3Sn_4 growth directions (converging and diverging) and a relatively wide spacing between the Ni_3Sn_4 rods. When it grows by divergence, the spacing becomes wider and wider. Once the spacing equals some branching limit, the Ni_3Sn_4 rod either branches to reduce the spacing or a new Ni_3Sn_4 crystal nucleates in the liquid ahead of the front. When it grows with convergence, the spacing becomes smaller and smaller. In this case, one of rods must stop growing to increase the spacing and the other rods keep growing, and thus overgrowth occurs. Additionally, it can be seen in Fig.5(a) that the Ni_3Sn_4 rods lead the βSn phase as is common for the faceted phase in nf-f eutectics. It can also be seen that the βSn front is at a similar z-position (i.e. growth temperature) in regions where there is a very wide local spacing and where there is a narrow local spacing. This occurs because the Sn liquidus line is very shallow in the Sn-Ni system so a build-up of Ni solute at the βSn-L interface does not cause a significant solute undercooling.

The significant 'irregularity' of the Sn-Ni_3Sn_4 eutectic front suggests that it has kinetic growth difficulties and, therefore, a relatively steep growth undercooling versus interface velocity relationship, which can partly explain why it can be out-competed by the metastable Sn-$NiSn_4$ eutectic when the velocity is increased. The particularly low critical velocity for the stable to metastable eutectic growth transition in Fig.3 is mostly due to the very small temperature difference between the stable and metastable equilibrium temperatures [1][2].

For comparison, a snapshot from the real time imaging of L = Sn + Ag_3Sn + Cu_6Sn_5 ternary eutectic growth in Sn-3.73Ag-0.85Cu is shown in Fig.5(b). The Cu_6Sn_5 rods are dark grey and the Ag_3Sn plates are light grey. A major differences between the eutectics is the fraction of the intermetallic phases in the eutectic mixture, which is much higher in the Sn-Ag-Cu alloy. Additionally, this eutectic is much better

aligned with the growth direction and is much less 'irregular' than the Sn-Ni_3Sn_4 eutectic in Fig.5(a) even though both Ag_3Sn and Cu_6Sn_5 are faceted phases. For example, the faceted Ag_3Sn-L interfaces can be seen clearly at the eutectic front in Fig.5(b). Additionally, it can be seen that the Cu_6Sn_5 rods and Ag_3Sn plates lead the βSn phase similar to the Sn-Ni_3Sn_4 eutectic in Fig.5(a).

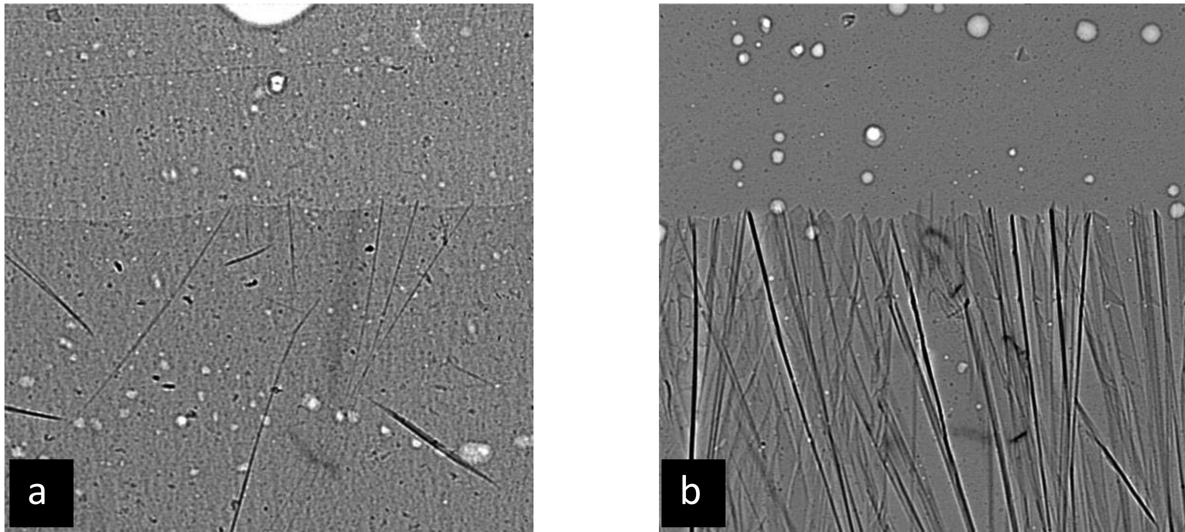

Fig.5. Typical growth fronts at 1 μm/s and 5 K/mm for (a) the stable Sn-Ni_3Sn_4 binary eutectic and (b) the Sn-Ag_3Sn-Cu_6Sn_5 ternary eutectic

Next Steps :

We are currently performing analytical SEM on the synchrotron samples so that we can identify the crystallography of eutectic growth and link that with the in-situ imaging. For example, EBSD analysis is being used to understand the growth directions of the faceted intermetallics, the Ni_3Sn_4 branching mechanisms (twinning, bending etc.) and to test for orientation relationships that develop during growth. With the knowledge of how the growth front was behaving at the location of the EBSD analysis, deeper understanding of the spacing selection mechanisms and of the eutectic 'regularity' can be extracted.

Acknowledgements :

Experiments were conducted at the Japan Synchrotron Radiation Research Institute (JASRI) on BL20XU under Proposal No. 2015B1611. Analysis was carried out under the Grant EP/K026763/1 (EPSRC).

References :

[1] Belyakov S.A., Gourlay C.M., *Intermetallics*, **25**, 48-59 (2012).
[2] Belyakov S.A., Gourlay C.M., *Intermetallics*, **37**, 32-41 (2013).
[3] Belyakov SA, Gourlay CM., *Materials Letters*, **148**, 91-5 (2015).
[4] H. Yasuda et al., *Journal of Crystal Growth*, **262**, 645-652 (2004).
[5] C.M. Gourlay et al., *Acta Materialia*, **59**, 4043-4054 (2011).